Optimizing a Phase Gate Using Quantum Interference

Eric Charron,[1] Eite Tiesinga,[2] Frederick Mies,[2] and Carl Williams[2]

[1]*Laboratoire de Photophysique Moléculaire du CNRS, Université Paris XI, 91405 Orsay Cedex, France*
[2]*Atomic Physics Division, NIST, 100 Bureau Drive Stop 8423, Gaithersburg, Maryland 20899-8423*

(Received 16 July 2001; revised manuscript received 21 November 2001; published 29 January 2002)

A controlled interference is proposed to reduce, by two orders of magnitude, the decoherence of a quantum gate for which the gate fidelity is limited by coupling to states other than the $|0\rangle$ and $|1\rangle$ qubit states. This phenomenon is demonstrated in an ultracold neutral atom implementation of a phase gate using qubits based on motional states in individual wells of an optical lattice.

DOI: 10.1103/PhysRevLett.88.077901 PACS numbers: 03.67.Lx, 32.80.Pj, 32.80.Qk

The controlled manipulation of quantum coherence and entanglement has fundamental physical interest and possible revolutionary applications to quantum information and computing [1]. The rapid development of quantum information has been stimulated by the discovery of a quantum factorization algorithm by Shor [2] and by the realization that, at the rate predicted by Moore's law, semiconductor technologies will soon reach the quantum limit. In addition to the experimental challenge [3] of realizing a physical system of many qubits whose evolution and interaction can be controlled at the quantum level, fulfilling these promises will require practical ways to minimize, or at least correct for, decoherence. Error correcting codes [1] provide recovery mechanisms when a given quantum state is perturbed by noise or unwanted interactions. These codes use redundancy by encoding the quantum state information into higher dimensional Hilbert spaces and are therefore expected to introduce additional complexity. Consequently, it is essential to reduce and control errors as much as possible for elementary two-qubit gate operations.

In this Letter, we propose an interference scheme aimed at improving the fidelity of a conditional phase gate by canceling excitation to quantum states residing outside the two-qubit subspace. We describe this quantum control scheme using the example of ultracold neutral atoms in optical lattices. Nevertheless, due to its general nature, this interference could be implemented in other proposals of elementary quantum logic devices where a conditional phase gate is used as one of the necessary building blocks of a universal quantum computer. These proposals include scenarios based on nuclear magnetic resonance [4], trapped ions [5], cavity quantum electrodynamics [6], and neutral atoms [7].

A conditional phase gate $P(\phi)$ induces entanglement between two qubits by changing the state $|11\rangle$ into $e^{i\phi}|11\rangle$, while leaving other states unchanged. In practice, it is often simpler to implement a phase gate which changes the states $|ab\rangle$ into $e^{i\phi_{ab}}|ab\rangle$, where a and b are the qubit labels 0 and 1. This transformation can be reduced to the conditional phase gate $P(\phi)$, with $\phi = \phi_{00} - \phi_{01} - \phi_{10} + \phi_{11}$, by using additional single-qubit operations. The case $\phi = \pi$ is of particular interest since $P(\pi)$ together with two one-qubit Hadamard gates form a controlled-NOT [1].

Our implementation of the phase gate uses qubits based on the external degrees of freedom of ultracold ground-state ^{87}Rb atoms in an optical lattice. Linearly polarized counterpropagating beams from the fundamental and first harmonic of a CO_2 laser produce an intensity gradient optical lattice along the x direction [see Fig. 1(a)] [8]. Along the other directions, y and z, an independent optical or magnetic trap is applied. Far from atomic resonance, the atomic polarizability is frequency independent and the associated periodic atomic trapping potential along the x direction is a succession of double minima separated by high barriers [see Fig. 1(b)]. With realistic CO_2 laser intensities, this structure supports a few motional states [9]. A single ^{87}Rb atom is trapped in each well. The interaction

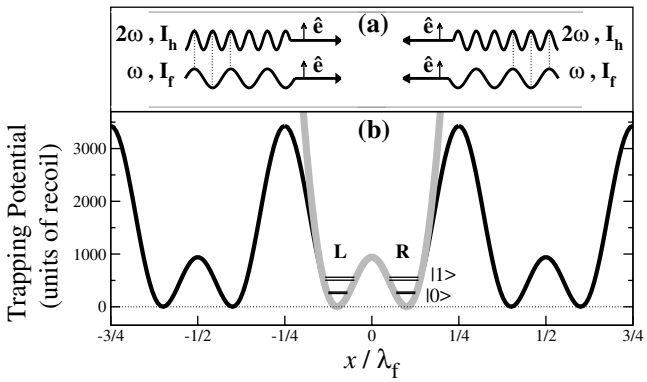

FIG. 1. Schematic picture of the neutral-atom optical lattice implementation. (a) Counterpropagating laser beams of frequencies ω and 2ω, intensities I_f and I_h, same linear polarization ê, and wavelengths $\lambda_f = 10.6\ \mu$m and $\lambda_h = 5.2\ \mu$m. (b) Black line: Optical lattice potential seen by the neutral atoms in units of the photon recoil energy $2\pi^2\hbar^2/m\lambda_f^2 \simeq 130$ Hz, where m is the ^{87}Rb mass. This trapping potential is proportional to the square of the electric field $I_f \cos^2(2\pi x/\lambda_f) + I_h \cos^2(2\pi x/\lambda_h)$. Grey line: Approximate optical potential used in this calculation. The energies of the first four motional states of a single atom in the double-well structure are drawn as thin horizontal lines. The two lowest states are indistinguishable on the scale of the figure. The left and right wells are denoted by L and R.

between atoms trapped in different double-well structures is negligible. Our model is therefore restricted to the two atoms trapped in a given double well. The confinement along y and z is assumed to be much stronger than the one along the x axis, such that during the gate operation the atoms stay in the lowest vibrational state along the y and the z directions. We therefore treat only the dynamics of the two atoms along x.

For numerical convenience, the periodic trapping potential along x is represented as the lower adiabat of a system of two coupled harmonic oscillators shown as the grey curve in Fig. 1(b). This figure also shows the energies of the lowest four eigenstates of a single atom trapped in the double-well potential. The corresponding eigenfunctions spread over both the left (L) and right (R) wells with either even or odd inversion symmetry with respect to $x = 0$. When the left and right wells are separated by a high barrier, tunneling is negligible and the atomic motional states can equally well be represented by wave functions which are localized in one of the wells. The two lowest motional states of each well define the qubit states $|0\rangle$ and $|1\rangle$.

In the present scheme, entanglement is due to atom-atom interactions caused by van der Waals and chemical forces. This interaction is typically of a much shorter range than the extent of the motional state wave functions, and can consequently be thought of as a three-dimensional delta-function potential with a strength proportional to the scattering length [10,11].

The effect of the atom-atom interaction is negligible when the barrier is high since the atomic wave functions do not overlap. However, when the barrier is lowered tunneling takes place and the energy shift due to the atom-atom interaction increases exponentially. The height of the barrier is controlled by the ratio of intensities $\alpha(t) = I_h/I_f$. It is natural to compose the phase gate out of three stages [see Fig. 2(a)]: $\alpha(t)$ first decreases from α_0 where the barrier is high, to α_1 where the barrier is low, between times $t = 0$ and $t = T_1$. Between $t = T_1$ and $t = T_1 + T_2$ the barrier is fixed at its lowest value, with $\alpha(t) = \alpha_1$. Finally, between $t = T_1 + T_2$ and $t = t_f = 2T_1 + T_2$, $\alpha(t)$ increases by reversing the $\alpha_0 \rightarrow \alpha_1$ sequence. Figure 2(b) shows the trapping potential for the two extreme cases $\alpha = \alpha_0$ and $\alpha = \alpha_1$.

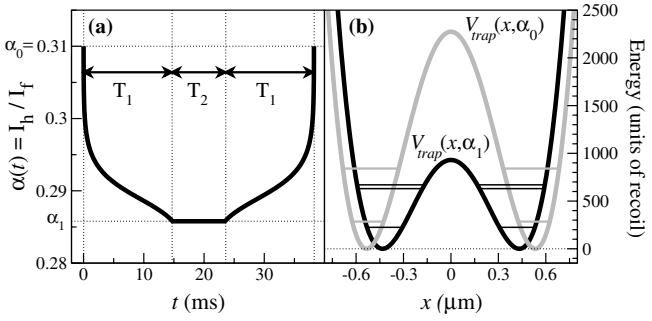

FIG. 2. Operation of the phase gate. (a) Variation of $\alpha(t) = I_h/I_f$ with time between $\alpha_0 = 0.310$ and $\alpha_1 = 0.286$ during the gate operation. (b) Associated trapping potential $V_{trap}(x, \alpha)$ for the highest ($\alpha = \alpha_0$, grey line) and lowest ($\alpha = \alpha_1$, black line) barrier heights. The trapping frequency ω_e of the wells varies between 60 and 80 kHz during the gate operation. The thin horizontal lines represent the four lowest eigenenergies of a single atom.

The entanglement is simulated by solving the time-dependent Schrödinger equation along the double-well direction for the wave packet $\Psi(x_1, x_2, t)$ describing the two atoms,

$$i\hbar \frac{\partial \Psi(x_1, x_2, t)}{\partial t} = \hat{\mathcal{H}}\big(x_1, x_2, \alpha(t)\big)\Psi(x_1, x_2, t), \quad (1)$$

where x_1 and x_2 are their respective positions. The Hamiltonian $\hat{\mathcal{H}}(x_1, x_2, \alpha)$ can be written as a sum of two single atom Hamiltonians $\hat{h}(x_1, \alpha) + \hat{h}(x_2, \alpha)$ and the atom-atom interaction $V_{\rm int}(|x_2 - x_1|)$, where

$$\hat{h}(x, \alpha) = -\frac{\hbar^2}{2m}\frac{d^2}{dx^2} + V_{\rm trap}(x, \alpha), \quad (2)$$

and $V_{\rm trap}(x, \alpha)$ describes the double well of Fig. 2(b). The interaction $V_{\rm int}(|x_2 - x_1|)$ can be obtained by averaging the three-dimensional delta function over y and z assuming that both atoms are in the lowest trap state along these directions [7]. The effective interaction becomes a one-dimensional delta function [10]. However, for numerical convenience this delta function is replaced by a Gaussian potential centered around $x_2 = x_1$. The strength and width of the Gaussian are chosen to mimic the effects of the repulsive delta-function potential.

Equation (1) is solved by expanding the wave packet $\Psi(x_1, x_2, t)$ in the time-dependent basis,

$$\Psi(x_1, x_2, t) = \sum_m c_m(t)\chi_m\big(x_1, x_2; \alpha(t)\big), \quad (3)$$

where $\chi_m\big(x_1, x_2; \alpha(t)\big)$, $m = 1, 2, \ldots$ are the adiabatic energy-ordered eigenstates of the Hamiltonian $\hat{\mathcal{H}}(x_1, x_2, \alpha)$ at $\alpha = \alpha(t)$, with the associated eigenenergies $E_n(\alpha)$. Inserting this expansion into Eq. (1) yields a set of coupled equations for the coefficients $c_n(t)$:

$$i\hbar \frac{dc_n}{dt} = E_n(\alpha)c_n(t) - i\hbar \frac{d\alpha}{dt}\sum_m V_{nm}(t)c_m(t), \quad (4)$$

where the time-dependent nonadiabatic couplings $V_{nm}(t)$ are the spatial integrals $\langle \chi_n | \partial/\partial\alpha | \chi_m \rangle$. Equation (4) is solved using a variable time step and variable order Runge-Kutta integrator [12].

Figure 3 shows two states χ_n for the maximum barrier height. These two states have one degree of excitation along each of the two directions x_1 and x_2. In panels (a), the wave function is localized around $x_1 \approx -x_2$, implying that the two atoms are trapped in different wells. This wave function therefore corresponds to the two-qubit state $|11\rangle$. The wave function shown in the other panel is localized

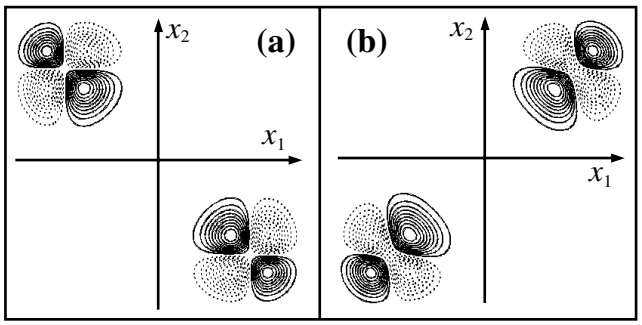

FIG. 3. Contour plots of two eigenstates $\chi_n(x_1, x_2; \alpha_0)$ when the barrier is high ($\alpha = \alpha_0$) as a function of the atom coordinates x_1 and x_2. The states $|11\rangle$ and $|\overline{11}\rangle$ are shown in panels (a) and (b), respectively. The solid and dotted contours represent positive and negative values. Note that because ^{87}Rb is a boson, the wave functions are symmetric under interchange of x_1 and x_2.

around $x_1 \approx x_2$ and is therefore an unwanted state where the two atoms are localized in the same well. This state is denoted by $|\overline{11}\rangle$. Similarly, each two-qubit state $|ab\rangle$ is associated with a state $|\overline{ab}\rangle$ which has the same degree of motional excitation but a slightly higher energy due to the larger atom-atom repulsion when the atoms are trapped in the same well. This interaction splitting is much smaller than the trapping frequency.

The operation of the quantum phase gate critically depends on the shape of $\alpha(t)$. In order to guarantee that the two-qubit states $|ab\rangle$ are restored up to a phase factor at the end of the gate, it is natural to choose $\alpha(t)$ such that the wave packet dynamics is nearly adiabatic. This near adiabatic behavior is achieved when the second term of the right-hand side of Eq. (4) is negligible compared to the first term. In practice, we keep the rate of change of $\alpha(t)$ small by imposing $\hbar|(d\alpha/dt)V_{nm}(t)| \leq \sigma|E_n(\alpha) - E_m(\alpha)|$ for all pairs of quantum states (n, m), where n is the index of a two-qubit state and $m \neq n$. The degree of adiabaticity is determined by the adjustable parameter $\sigma \ll 1$. A typical shape of $\alpha(t)$, obtained for $\sigma \approx 0.05$, is shown in Fig. 2(a).

The variation with time of $\alpha(t)$ can be explained on physical grounds. At early times ($t \simeq 0$), the barrier is high and the states $|ab\rangle$ and $|\overline{ab}\rangle$ are localized in different regions of space (see Fig. 3, for instance). Consequently, a two-qubit state $|ab\rangle$ is mostly coupled to states with a different vibrational excitation rather than to its almost degenerate companion $|\overline{ab}\rangle$, and the barrier separating the two wells can drop relatively quickly compared to the inverse of the level spacing between the $|ab\rangle$ and $|\overline{ab}\rangle$ states. However, the time scale of this variation must still be slow compared to the trap oscillation period. At later times ($t > 0.1T_1$), tunneling begins and the states $|ab\rangle$ and $|\overline{ab}\rangle$ become more strongly coupled. Consequently, the decrease of the barrier separating the two wells must occur at a smaller rate. Out of the four two-qubit states, $|11\rangle$ is most strongly affected by tunneling, which results in the largest nonadiabatic couplings $V_{nm}(t)$. This state thereby constrains the gate operation.

Consequently, the fidelity $\mathcal{F}$ could be defined as the probability $P_{|11\rangle}(t_f) = |c_{11}(t_f)|^2$ of remaining in the initial state $|11\rangle$ at the end of the gate. In general, the fidelity is defined as $\mathcal{F} = \sum_{a,b} P_{|ab\rangle}(t_f)$, and the quantity $(1 - \mathcal{F})$ therefore measures the deviation from adiabaticity, which arises from the nonadiabatic couplings induced by the lowering and raising portions of $\alpha(t)$. We can thus increase the fidelity by increasing T_1, but only at the sacrifice of increasing the gate duration. An estimate based on perturbation theory suggests that for $(1 - \mathcal{F}) \approx 10^{-3}$ the phase $\phi = \pi$ requires a minimum gate duration t_f of about 25 ms. The same analysis indicates that improving the fidelity to $(1 - \mathcal{F}) \approx 10^{-5}$ requires increasing T_1 by a factor of 10. This yields a very slow gate, of duration of the order of 250 ms. A numerical simulation gives a fidelity of $(1 - \mathcal{F}) \approx 2 \times 10^{-5}$ with these parameters. However, this analysis assumes that the nonadiabatic populations produced when lowering and raising the barrier simply add up. Fortunately, an interference can be used to dramatically improve the gate fidelity without significantly increasing its duration.

Figure 4 shows the final $|\overline{ab}\rangle$ population for initial states $|ab\rangle = |00\rangle$, $|01\rangle$, $|10\rangle$, and $|11\rangle$ as a function of t_f. The gate duration t_f is varied by increasing T_2 for fixed T_1. Each curve oscillates or beats with a distinct oscillation period $\tau = 2\pi\hbar/[E(|\overline{ab}\rangle) - E(|ab\rangle)]$ imposed by the energy difference between the two coupled states $|ab\rangle$ and $|\overline{ab}\rangle$ at the minimum barrier height. For a given state $|ab\rangle$, constructive interference yields a maximum population transfer in the unwanted state $|\overline{ab}\rangle$, while destructive interference leads to a minimum excitation probability. Note that excitation to other motional states, although explicitly included in the calculation, are negligible and at most of the order of 10^{-7}.

A schematic of this interference, based on first-order perturbation theory, is shown in Fig. 5 for the initial state $|11\rangle$. This figure shows the coefficients $c_n(t)$ of the adiabatic eigenstates $|11\rangle$ and $|\overline{11}\rangle$ during the gate operation,

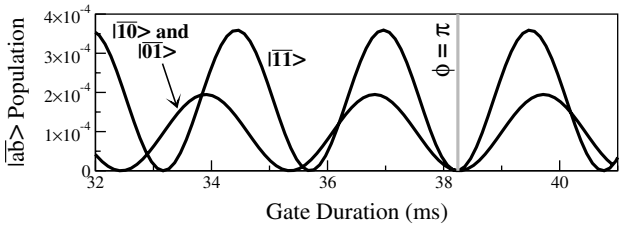

FIG. 4. Population exited in the state $|\overline{ab}\rangle$ at the end of the gate as a function of the gate duration when the initial state at time $t = 0$ is the two-qubit state $|ab\rangle$. The populations excited in the states $|\overline{01}\rangle$ and $|\overline{10}\rangle$ are nearly indistinguishable, and the population of $|\overline{00}\rangle$ is negligible on the scale of this figure. The vertical grey line indicates the gate duration for which a phase $\phi = \pi$ is accumulated.

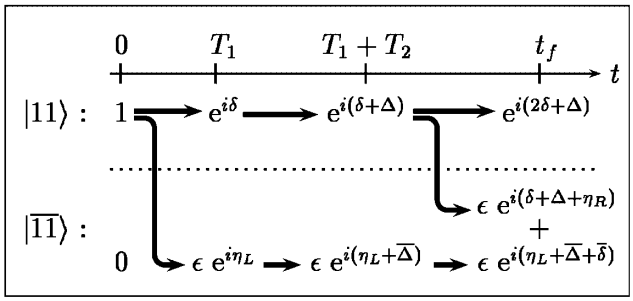

FIG. 5. Evolution of the coefficients $c_n(t)$ corresponding to the states $|11\rangle$ and $|\overline{11}\rangle$ as a function of time t, ignoring second order processes. The initial two-qubit state is $|11\rangle$.

where we should recall that these states are implicit functions of time. As a result of the nonadiabatic couplings introduced when lowering the barrier, the wave packet $\Psi(t)$ of Eq. (3) emerges at time $t = T_1$ with a small but undesirable amplitude $\epsilon \ll 1$ in state $|\overline{11}\rangle$, while the amplitude in $|11\rangle$ is close to 1. The associated phases developed by these two states are denoted by δ and η_L. During the interval $T_1 \leq t \leq T_1 + T_2$, the Hamiltonian is time independent, and since $|11\rangle$ and $|\overline{11}\rangle$ are exact eigenfunctions of this Hamiltonian their amplitudes evolve separately, each accumulating an additional phase $\Delta = -E(|11\rangle)T_2/\hbar$ and $\overline{\Delta} = -E(|\overline{11}\rangle)T_2/\hbar$. Finally, the barrier is raised between times $t = T_1 + T_2$ and $t = t_f$. At time t_f, the state $|11\rangle$ emerges with a near unity amplitude and a phase $2\delta + \Delta$, while simultaneously producing a nonadiabatic contribution $\epsilon e^{i(\delta+\Delta+\eta_R)}$ to the $|\overline{11}\rangle$ component. The other $|\overline{11}\rangle$ component, produced when lowering the barrier, acquires the additional phase $\overline{\delta}$ when raising the interwell potential.

There are thus two distinct pathways leading to the state $|\overline{11}\rangle$, depending on whether the excitation takes place when lowering or raising the barrier. Note that since these two operations are symmetric under time reversal, they induce an *equal* amplitude ϵ in the unwanted state $|\overline{11}\rangle$. These two amplitudes interfere and yield the oscillation of the $|\overline{ab}\rangle$ populations seen in Fig. 4.

Since this control scenario uses a symmetric sequence of transformations, it has some similarities with Ramsey's separated oscillatory fields method for atomic clocks [13], as well as with solid state NMR control fields used to selectively turn off persistent couplings between nearby spins [14]. Here, the first and last steps of the gate constitute the two arms of an interferometer. By controlling the phase relation between these two arms, the unwanted states can be depopulated. A specific $\alpha(t)$ is required in order to impose destructive interference for all four two-qubit states simultaneously, and at a time when the accumulated phase ϕ equals π. The $\alpha(t)$ which is shown in Fig. 2(a) has been optimized to satisfy this criterion and has been used to obtain Fig. 4. This gate has a duration of 38 ms and is therefore only 50% slower than the 25 ms gate described previously, with a fidelity improved by more than 2 orders of magnitude, i.e., $(1 - \mathcal{F}) \approx 6.3 \times 10^{-6}$.

In this Letter we have shown that it is possible to avoid decoherence into a few nearby quantum states during the operation of a two-qubit phase gate using a quantum interference scheme. We have applied this scheme to a gate based on the motional states of neutral atoms trapped in an optical lattice. The proposed scenario can cancel undesired population transfer when the decoherence dynamics is accurately described by first-order perturbation theory. This is obviously not a serious limitation since almost all proposed phase gates rely on a nearly adiabatic transformation [1]. Furthermore, this scheme requires the gate to be implemented in three *symmetric* steps consisting in (i) switching on the qubit interaction, (ii) letting the interaction perform for a time, and (iii) switching off the interaction. This is again compatible with the implementation of most phase gates. This suggests that the proposed scenario has a wide range of possible applications. For instance, in neutral atom proposals based on internal states, it is difficult to limit motional state excitation [7], and ion traps have similar limits due to nearby center-of-mass motional states [5].

[1] A. Steane, Rep. Prog. Phys. **61**, 117 (1998).
[2] P. Shor, in *Proceedings of the 35th Annual Symposium on Foundations of Computer Science* (IEEE Computer Society Press, Los Alamitos, CA, 1994).
[3] P. Divincenzo, Fortschr. Phys. **48**, 771 (2000).
[4] J. Jones, Prog. Nucl. Magn. Reson. Spectrosc. **38**, 325 (2001).
[5] I. Cirac and P. Zoller, Phys. Rev. Lett. **74**, 4091 (1995); C. Monroe *et al., ibid.* **75**, 4714 (1995); I. Cirac and P. Zoller, Nature (London) **404**, 579 (2000).
[6] Q. Turchette *et al.,* Phys. Rev. Lett. **75**, 4710 (1995); A. Rauschenbeutel *et al., ibid.* **83**, 5166 (1999).
[7] D. Jaksch *et al.,* Phys. Rev. Lett. **82**, 1975 (1999); G. Brennen *et al., ibid.* **82**, 1060 (1999); D. Jaksch *et al., ibid.* **85**, 2208 (2000); A. Hemmerich, Phys. Rev. A **60**, 943 (1999); T. Calarco *et al., ibid.* **61**, 022304 (2000); G. Brennen *et al., ibid.* **61**, 062309 (2000).
[8] L. Guidoni and P. Verkerk, J. Opt. B **1**, R23 (1999).
[9] S. Friebel *et al.,* Phys. Rev. A **57**, R20 (1998).
[10] T. Busch *et al.,* Found. Phys. **28**, 549 (1998).
[11] E. Tiesinga *et al.,* Phys. Rev. A **61**, 063416 (2000); P. S. Julienne *et al.,* Phys. Rev. Lett. **78**, 1880 (1997).
[12] R. Brankin *et al., Contributions to Numerical Mathematics,* edited by R. Agarwal (World Scientific, Singapore, 1993), p. 41.
[13] J. Vanier and C. Audoin, *The Quantum Physics of Atomic Frequency Standards* (Hilger, Bristol, 1989).
[14] D. W. Leung *et al.,* Phys. Rev. A **61**, 042310 (2000); L. Tian and S. Lloyd, *ibid.* **62**, 050301 (2000).